21, rue d'Artois, F-75008 PARIS
http : //www.cigre.org

2016 CIGRE International Colloquium

No-load Voltage Waveform Analysis of Large Tubular Hydro-generator under Damper Bar Broken Down Failure

Z. GUANGHOU [1,2], H. LI[2], F. ZHENNAN [3*], L. JIANFU [1]

[1]Dongfang Electrical Machinery Company Limited
[2] Chongqing University
[3]Xihua University
China

SUMMARY

To ensure the power quality and provide more references for the detection of damper bar broken down failure in tubular hydro-generators, the no-load voltage waveforms of a generator under damper bar broken down failure are analyzed and calculated by 3D multi-slice moving electromagnetic field-circuit coupling model in detail. And then, important parameters to the no-load voltage waveform quality are discussed, such as the harmonic distortion factor (HDF), the telephone harmonic factor (THF) and the tooth harmonics. Furthermore, the influences of different structures are considered, such as stator slots skew, damper winding shift and pole shoes shift. The research of this paper is helpful to improve the power quality and provide more effective references for the detection of this kind of failure in the tubular hydro-generator.

KEYWORDS

No-load voltage waveform, Large tubular hydro-generator, Damper bar broken down failure

fanzhennan@126.com

1. INTRODUCTION

The no-load voltage waveform quality has important influence on the security of grid connection and operation of hydro- generator. And the damper bar structure condition has important influence on the generator no-load voltage waveform quality [1]. In recent years, a real special kind of damper bar broken-down failure frequently occurred in some large tubular hydro-generators at different hydropower stations[2]. This kind of failure has two main features. Firstly, the damper bar broken-down failure occurrd at almost all poles of the tubular hydro-generators. Secondly, all the damaged bars were always located near the leeward area of the pole, as shown in Fig. 1. Therefore, to ensure the no-load voltage waveform quality and power quality, to provide more concise and effective references for the detection of the damper bar broken-down failure, it is necessary to study the no-load voltage waveform of tubular hydro-generator under this special failure in detail.

For the calculation and the analysis of hydro-generator no-load voltage waveform, some fruitful researches were carried out for the hydro-generators which damper bars in normal condition.[3] used the early analytical formula to analyze and improve the performance of the no-load voltage waveform by the methods of increasing air gap, using fractional slot, skewing the stator slot or rotor pole, improving the surface shape of pole shoe, moving the pole position, changing the structure of damper bars. In recent years, the magnetic field and harmonic voltage of salient pole generators were calculated and analyzed by 2D finite element (FE) method or field-circuit coupling method, and the influence of the some structure parameters were discussed [4-6]. [6] analyzed the influence of damper bar pitch and stator slot skewing degree on the no-load voltage waveform of the healthy tubular hydro-generator in detail by the multi-slice moving electromagnetic field-circuit coupling model. However, the study of the no-load voltage waveform under the special damper bar broken-down failure in [6] was absent.

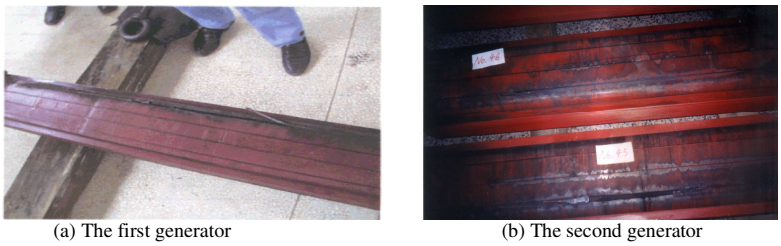

(a) The first generator (b) The second generator

Fig. 1 Damaged damper bars in different tubular hydro-generators

On the study about the detection of the broken bar failure, though abundant achievements have been obtained for induction machines with squirrel cage bars [7]-[8], however, the study on the tubular hydro-generators with damper bars is seldom. In [9], the flux probe measurement and time-stepping FE analysis were used to detect the damper bar broken-down failure in a pumped storage hydro-generator. In [10], a novel analytical method for predicting the broken bar fault signature amplitude in synchronous machine damper winding was proposed. In [11], a new robust method was applied to detect the damaged damper bars in salient- pole synchronous machines. In [12], a method of modeling synchronous machines with damper windings based on the winding function approach was proposed, and its model can be used to simulate the generator under the damper bar broken- down condition. However, the no-load voltage waveform quality, such as HDF and THF information, for the detection of the damper bar broken-down failure still needs to be researched and provided in detail.

Furthermore, to ensure the no-load voltage quality and provide more references for the detection of the special damper bar broken-down failure in tubular hydro-generator, the no-load voltage waveform of the generator under this failure need to be studied from the following two aspects. Firstly, the influences of the different structure design schemes should be considered more comprehensive, such as the stator slot skew, the damper bar and the pole shoe shift. Secondly, it is necessary to strengthen the analysis of the harmonic voltages.

Aiming the above goals, the no-load voltage waveforms of a tubular hydro-generator under the damper bar broken-down failure are calculated and analyzed in this paper. And the accuracy and rationality of the calculation are verified by the voltage test.

2.CACLULATION MODELS

2.1.The main features of the damper bar broken-down failure of the tubular hydro-generator

The damper bar broken-down failure discussed in this paper has the following main features. Firstly, all the poles have damaged damper bars. Secondly, all the damaged bars are located near the leeward area of the pole, as shown in Fig. 1.

In the discussion of this paper, the different structure design schemes of the generator are shown in TABLE I， in which t_1 is the stator tooth pitch.

TABLE I

DIFFERENT STRUCTURE DESIGN SCHEMES OF THE GENERATOR

Structure scheme	Description
1	Pole shoe and damper bar no shift, stator slot no skew
2	Pole shoe and damper bar shifted $0.25t_1$, stator slot no skew
3	Pole shoe and damper bar no shift, stator slot skewed $0.5\ t_1$
4	Pole shoe and damper bar no shift, stator slot skewed t_1

The geometric structure of the pole and the damper bars are shown in Fig. 2. There are 6 damper bars on each pole shoe. For easy discussion, the damper bar on the leeward side is numbered as the 1st and the damper bar on the windward side is numbered the 6th.

Four different kinds of damper bar broken-down failures are discussed in this paper. Firstly, no bar broken-down occurs. Secondly, the 1st damper bar is broken-down per pole. Thirdly, the 1st and the 2nd damper bars are broken-down per pole. Fourthly, the 1st, the 2nd and the 3rd damper bars are broken-down per pole.

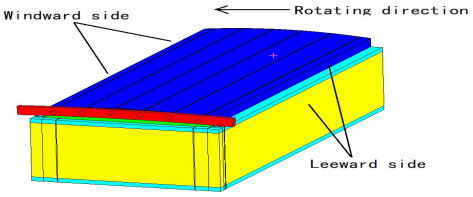

Fig. 2 The pole and damper winding

2.2. Basic parameters of the generator

The basic parameters of the tubular hydro-generator are tabled as follows.

TABLE II

BASIC DATA OF THE GENERATOR

Parameter	Value
Rated power P_N (MW)	34
Rated voltage U_N (kV)	10.5
Rated current I_N (A)	1968
Rated Power factor cos ϕ_N	0.95
Number of magnetic poles $2p$	44
Number of damper bars per pole N_b	6
Number of slots per pole per phase q	2

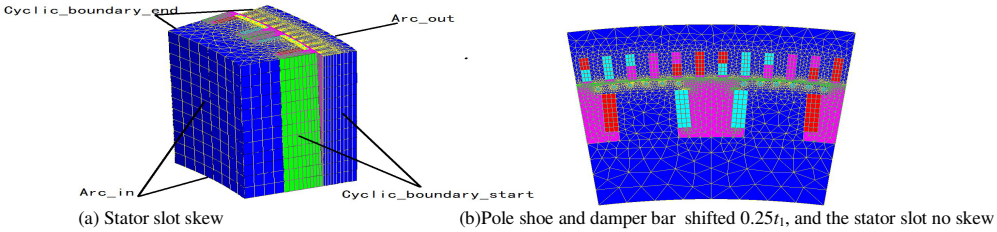

(a) Stator slot skew (b)Pole shoe and damper bar shifted $0.25t_1$, and the stator slot no skew

Fig. 3 The problem region and FE meshes of electromagnetic field

2.3. 3D multi-slice moving electromagnetic field-circuit coupling model of the generator

To consider the influence of the skewed stator slot structure, a 3D multi-slice moving electromagnetic field-circuit coupling model of the generator is built up.

According to the periodicity of the magnetic field, a pair of poles is chosen as the electromagnetic field calculation region. For the stator slot skewed structure design scheme, along the axial direction, the generator is divided into 12 equal slices. For the structure schemes without the stator slot skewed, the calculation region has only 1 slice, which is equivalent to a 2D electromagnetic field problem, as shown in Fig. 3.

Considering the saturation of iron core, the 3D boundary value problem of nonlinear time-varying electromagnetic moving field is obtained:

$$\begin{cases} \nabla \times (\nu \nabla \times \mathbf{A}) + \dfrac{1}{\rho}\left[\dfrac{\partial \mathbf{A}}{\partial t} - \mathbf{V} \times (\nabla \times \mathbf{A})\right] = \mathbf{J}_s \\ \mathbf{A}\big|_{Arc\_in} = \mathbf{A}\big|_{Arc\_out} = 0 \\ \mathbf{A}\big|_{Cyclic\_boundary\_start} = \mathbf{A}\big|_{Cyclic\_boundary\_end} \end{cases} \quad (1)$$

where $\mathbf{A}$ is the magnetic vector potential, $\mathbf{J_s}$ is the source current density, v is the reluctivity, $\mathbf{V}$ is the velocity and ρ is the resistivity.

For each slice, the current density and magnetic vector potential have only the axial z component, and the speed has only the circumferential x component. With the Coulomb norm $\nabla \cdot \mathbf{A} = 0$ and the boundary condition of the problem region, the 2D boundary value problem of nonlinear time-varying moving electromagnetic field for the generator is then obtained:

$$\begin{cases} \dfrac{\partial}{\partial x}(\nu \dfrac{\partial A_{slz}}{\partial x}) + \dfrac{\partial}{\partial y}(\nu \dfrac{\partial A_{slz}}{\partial y}) = -J_{slz} + \dfrac{1}{\rho}\dfrac{\partial A_{slz}}{\partial t} + \dfrac{V_x}{\rho}\dfrac{\partial A_{slz}}{\partial x} \\ A_{slz}\big|_{arc\_in} = A_{slz}\big|_{arc\_out} = 0 \\ A_{slz}\big|_{cyclic\_boundary\_start} = A_{slz}\big|_{cyclic\_boundary\_end} \end{cases} \quad (2)$$

where V_x is the circumferential component of velocity, J_{slz} and A_{slz} are the axial component of source current density and magnetic vector potential respectively.

To consider the influence of the stator end winding and the rotor damper winding end rings, the coupling circuit models are established,as shown in Fig.4 and Fig.5.

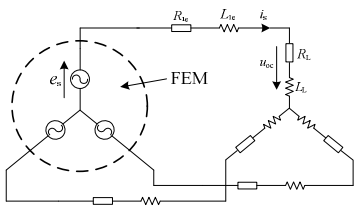

Fig. 4 Coupling circuit of the stator winding

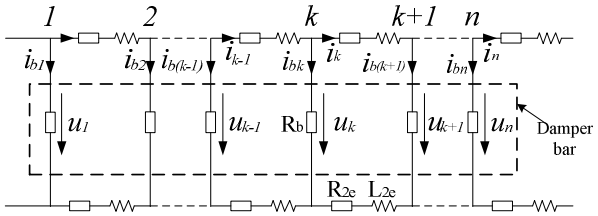

Fig. 5.Coupling circuit of the damper winding

The stator and rotor coupling circuit equations and the electro- magnetic equations are combined, the magnetic vector potential A_{slz} of slices is calculated by time-step FE method, and then the flux density and the voltage can be acquired.

3.THE CACLULATION RESULTS AND DISCUSSIONS

3.1.Verification of no-load voltage calculation

The no-load operating condition of the generator is simulated by setting the load resistance R_L and load inductance L_L to infinite in Fig. 4. And the damper bar broken-down failure is simulated by setting the resistivity of the damaged damper bars to infinite in Fig. 5. And then, the no-load voltage under the damper bar broken-down failure can be calculated by the FE calculation.

The above model settings indicate that,in this paper, both the normal condition and the bar broken condition,the no-load voltage is solved and analyzed by the same calculation model,and in the simulation, the difference between the above conditions only reflected by the different resistivity setting of the damaged bars.Therefore,although the hydropower station is not allow to damage the damper bars for the no-load voltage test,but the accuracy and rationality of calculation model can still be indirectly validated by the test of the no-load voltage under the normal conditions.

In the no-load voltage test and analysis, the deviation between the actual and sinusoidal waveforms of the line voltage is defined as the Harmonic Distortion Factor (HDF), whose value is defined according to the Chinese National Standard GB/T 1029-2005:

$$HDF = \frac{\sqrt{U_2^2 + U_3^2 + \cdots\cdots + U_n^2}}{U_1} \times 100\% \qquad (3)$$

And to weigh the disturbance for the harmonics of voltage waveform to telecommunication, the Telephone Harmonic Factor (THF) is defined as the following according to the GB/T 1029-2005:

$$THF = \frac{\sqrt{U_1^2\lambda_1^2 + U_2^2\lambda_2^2 + \ldots + U_n^2\lambda_n^2}}{U} \times 100\% \qquad (4)$$

where U is the actual line voltage, U_i (i=1, 2, 3, …, n; n is the highest order of harmonic considered) is the line voltage value of the k^{th} harmonic, and λ_k is the weighted coefficient of the k^{th} harmonic.

At the same time, in the no-load voltage test and analysis, the tooth harmonics should be considered. The ordinal number of tooth harmonics of voltage is given by:

$$\nu = k2mq \pm 1 \qquad (5)$$

where k is the order of tooth harmonic, m is the number of phases and q is the number of the slots per pole per phase. For the generator of TABLE II, q is 2, and the ordinal number of 1st and 2nd order tooth harmonics are 11th and 13th, 23th and 25th respectively.

In the no-load voltage test, the sampling time is set to 0.01 ms, and the harmonic frequency is taken at most 5 kHz.

The test scheme is shown in Fig.6 ,and the no-load voltage waveform and harmonics distribution are shown in Fig.7 and TABLE III.

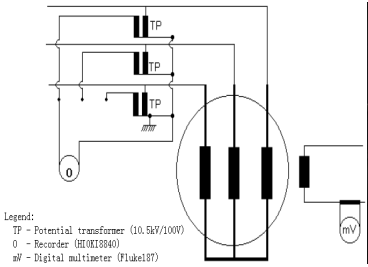

Fig. 6 Schematics of voltage waveforms test

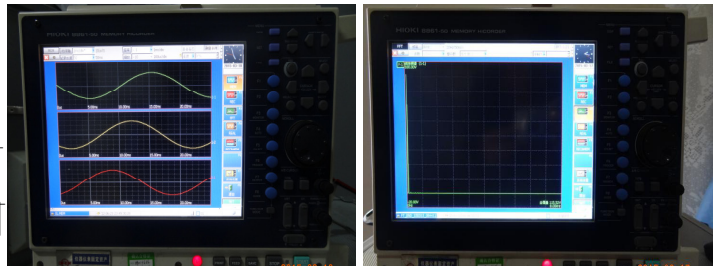

Fig. 7 The test waveform and harmonics

TABLE III
VERIFICATION OF RESULTS OF NO-LOAD VOLTAGE WAVEFORMS(U_{ab})

	Harmonics of the no-load voltage (%)					Voltage quality	
	1	11	13	23	25	*HDF*(%)	*THF* (%)
Calculated	100	1.512	0.799	0.044	0.150	1.843	1.172
Measured	100	1.550	0.816	0.039	0.161	1.850	1.186

The above results show that the simulation is well closed to the test, and they indicate that the accuracy and rationality of the calculation model of this paper are successfully verified. Therefore, the calculation and analysis results of this model can be considered to be accurate and reliable.

3.2. The no-load voltage waveform quality

Because of the symmetry of the no-load line-line voltages U_{ab}, U_{bc} and U_{ca}, this paper discusses only U_{ab}.The HDF, THF with different structure design schemes are shown as Fig. 8.

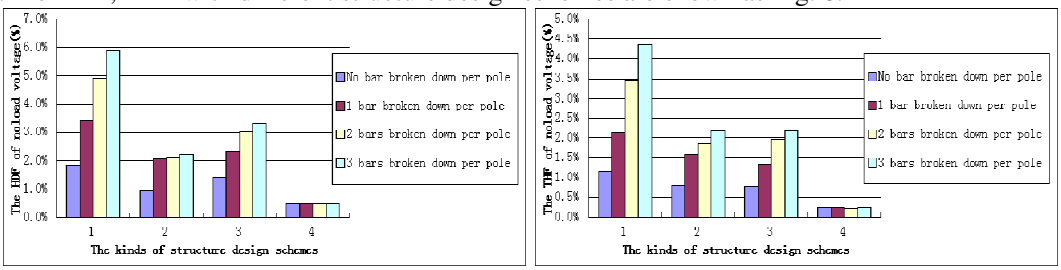

(a) The HDF (b) The THF

Fig. 8 The HDF and the THF of the different structure design schemes

Some important phenomena can be then obtained as follows by the above results :

① For the structure design scheme 1, 2 and 3, with the increase of the numbers of the broken-down bars per pole, the HDF and the THF of no-load voltage increase obviously, and the no-load voltage waveform quality becomes worse.

② For the structure design scheme 4, however, the HDF and the THF are almost constant with the change of the numbers of the broken-down bars per pole, i.e. the damage of damper bars does not affect the no-load voltage waveform quality.

③ The no-load voltage waveform can be optimized obviously by changing the structure design scheme from 1 to 2, 3 or 4. Comparison the scheme 2, 3 and 4, scheme 2 is simplest and most convenient for the manufacture.

④ Except for the structure design scheme 4, the no-load voltage waveform quality of other schemes will change after the damper bar broken-down failure. This result can provide an evident reference for the detection of the failure.

3.3. Harmonic analysis of the no-load voltage

To analyze the reason of the above results, the harmonic analysis of the no-load voltage are carried out. And in order to analyze the influence of the tooth harmonics on the HDF and the THF, the parameter F_n and T_n are defined respectively as follows.

$$F_n = \frac{\sqrt{U_{11}^2 + U_{13}^2 + U_{23}^2 + U_{25}^2}}{U_1} \times 100\% \qquad (6)$$

$$T_n = \frac{\sqrt{U_{11}^2 \lambda_{11}^2 + U_{13}^2 \lambda_{13}^2 + U_{23}^2 \lambda_{23}^2 + U_{25}^2 \lambda_{25}^2}}{U} \times 100\ \% \qquad (7)$$

Some results can then be obtained in Fig. 9 to Fig. 12.

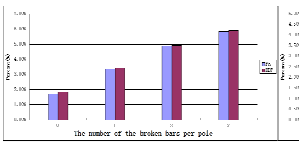

(a)F_n and HDF

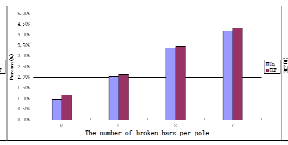

(b) T_n and THF

Fig. 9 Scheme 1

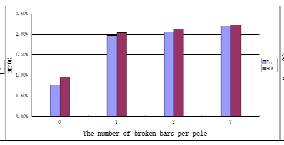

(a)F_n and HDF

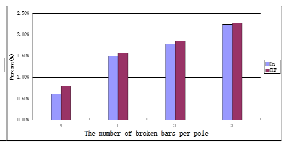

(b) T_n and THF

Fig. 10 Scheme 2

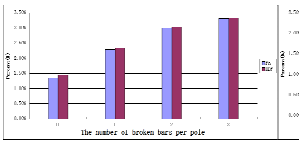

(a)F_n and HDF (b) T_n and THF

Fig. 11 Scheme 3

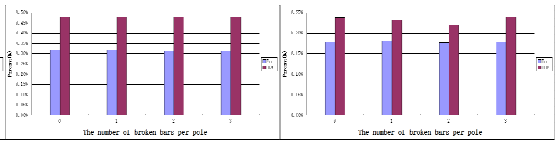

(a)F_n and HDF (b) T_n and THF

Fig. 12 Scheme 4

The results of Fig. 9 to Fig. 12 show that 1st and 2nd order tooth harmonics (11th and 13th, 23th and 25th) have decisive influences on the no-load voltage waveform.

After the analysis of the above tooth harmonics, the relation between the tooth harmonics and the number of broken-down bars per pole are obtained, as shown in Fig. 13.

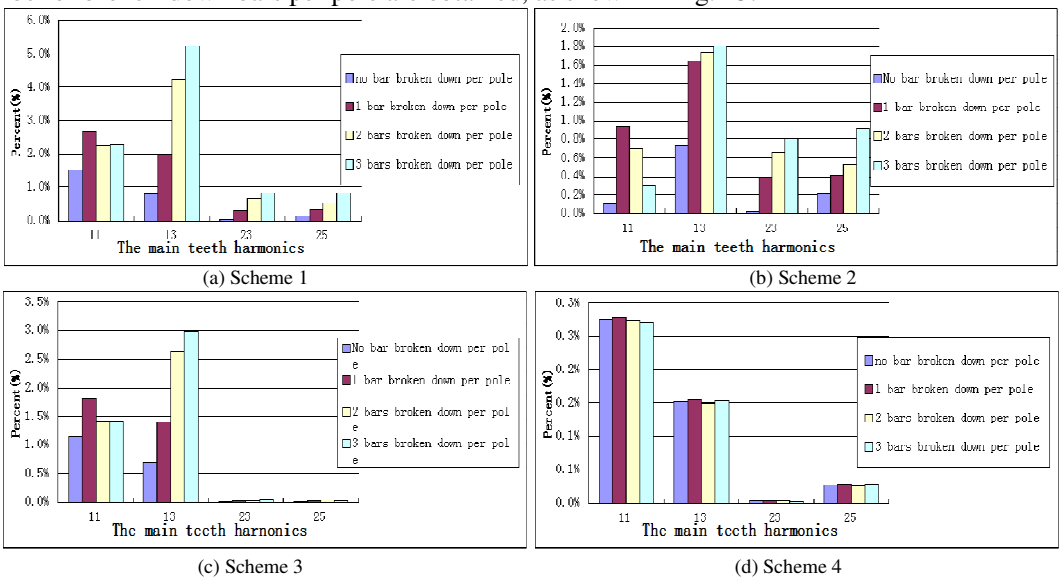

(a) Scheme 1 (b) Scheme 2

(c) Scheme 3 (d) Scheme 4

Fig. 13 The main tooth harmonics of the no-load voltage

Some phenomena can be then obtained by Fig. 13 :

① For the structure design scheme 1, 2 and 3, with the increase of broken-down bars per pole, the tooth harmonics increase obviously in total, so the HDF and the THF increase significantly, and the no-load voltage waveform quality becomes worse.

② The scheme 4 can weaken the tooth harmonics most effectively and can obtain the best no-load voltage waveform. However, the damper bar broken-down failure has almost no effect on its tooth harmonics, so the no-load voltage waveform quality is not affected.

③ For the scheme 1, 2 and 3, the damper bar broken-down failure can be detected by monitoring the HDF and the THF change of the no-load voltage.

4.CONCLUSION

For the tubular hydro-generator which the number of slots per pole per phase is 2 in this paper, both the pole shoe and damper winding shifted $0.25t_1$, and the stator slots skewed half or one t_1, can weaken the tooth harmonic effectively, so the better no-load voltage waveform can be obtained. Especially, if the stator skewed one t_1 scheme is adopted, the best waveform is obtained.

For the stator skewed one t_1 scheme, the damper bar broken down failure has almost no effect on its tooth harmonics, so its no-load voltage waveform quality is not affected.

And for the other structural design schemes, with the increasing of damaged bars per pole, the tooth harmonics are increased obviously in total, so the no-load voltage waveform quality becomes worse.

And the damper bar broken down failure can be detected by monitor the tooth harmonics of no-load voltage.

The accuracy and rationality of the calculation model in this paper are verified by voltage test. And the research of this paper is helpful for improve the power quality, and provide more effective references for the detection of this kind of failure in the tubular hydro-generator.

ACKNOWLEDGMENT

This work was sponsored by the Key Scientific Research fund project of Xihua University, No.Z1520907 and the Key Research fund projects of Si chuan Provincial Education Department No. 16ZA0155.

BIBLIOGRAPHY

[1] Chao-Yang Li, “The Application of Bulb-type Hydro-Generator Set at Low Head Hydropower Station,” *Developing*, no. 9, pp. 145-146, 2006.
[2] Jing-Bin Guo, “Analysis of Damaged Damping Winding and Magnetic Pole in Bulb Type Generator,” *Chinese Power*, vol. 34, no. 7, pp. 63-67, May 2001.
[3] Zhesheng Li, “Measurement of Improving No-load Voltage Waveforms of Salient-pole Synchronous Generator”, *Journal of Harbin Institute of Electrical Technology*, vol.6, no.3, pp.1-16, Sept 1983.
[4] ChangEobKim andJ.K. Sykulski, “Harmonic Analysis of Output Voltage in Synchronous Generator Using Finite Element Method Taking Account of the Movement,” *IEEE Trans. on Magnetics*, vol.38, no.2, pp.1249-1252, March 2002.
[5] Stefan Keller, Mai Tu Xuan, and Jean-Jacques Simond, “Computation of the No-Load Voltage Waveform of Laminated Salient-Pole Synchronous Generators,” *IEEE Trans. on Industry Applications*, vol.42, no.3, pp.681- 687, May/June 2006.
[6] Zhen-nan Fan, Yong Liao, Li Han, Li-dan Xie, "No-load Voltage Waveform Optimization and Damper Bars Heat Reduction of Tubular Hydro- Generator by Different Degree of Adjusting Damper Bar Pitch and Skewing Stator Slot"*, IEEE Trans. on Energy Conversion*, vol.28,no.3, pp.461-469,September, 2013.
[7] R. R. Schoen, T. G. Habetler, “Effects of time-varying loads on rotor fault detection in induction machines,” IEEE Transactions on Industry Applications, vol. 31, no. 4, pp. 900-906, July/August 1995.
[8] S. Nandi, H. A. Toliyat, X. Li, “Condition Monitoring and Fault Diagnosis of Electrical Motors-A Review,” IEEE Transactions on Energy Conversion, vol. 20, no. 4, pp. 719-729, Dec. 2005.
[9] Karmaker, H.C, “Broken damper bar detection studies using flux probe measurements and time-stepping finite element analysis for salient-pole synchronous machines,” in *Proc.* SDEMPED 2003. 4th IEEE International Symposium on, 2003, pp.193-197.
[10] Mina M. Rahimian, Seung Choi, Karen Butler-Purry, “A novel analytical method for prediction of the broken bar fault signature amplitude in induction machine cage rotor and synchronous machine damper winding,” in *Proc.* Energy Conversion Congress and Exposition (ECCE), 2011 IEEE，2011，pp.1641-1648.
[11] Prabhakar Neti,A. B. Dehkordi, A. M. Gole, “A New Robust Method To Detect Rotor Faults in Salient-Pole Synchronous Machines Using Structural Asymmetries,” in *Proc* .Industry Applications Society Annual Meeting, 2008. IAS '08. IEEE ， 2008，pp.1-8.
[12] Mina M. Rahimian, Karen Butler-Purry, “Modeling of synchronous machines with damper windings for condition monitoring,” in *Proc.* Electric Machines and Drives Conference, 2009. IEMDC '09. IEEE International, 2009，pp.577-584.